Dear Author

Please use this PDF proof to check the layout of your article. If you would like any changes to be made to the layout, you can leave instructions in the online proofing interface. Making your changes directly in the online proofing interface is the quickest, easiest way to correct and submit your proof. Please note that changes made to the article in the online proofing interface will be added to the article before publication, but are not reflected in this PDF proof.
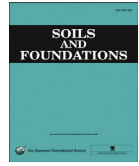
If you would prefer to submit your corrections by annotating the PDF proof, please download and submit an annotatable PDF proof by clicking here and you'll be redirected to our PDF Proofing system.

Interface shear strength characteristics of steel piles in frozen clay under varying exposure temperature ☆

Abdulghader A. Aldaeef, Mohammad T. Rayhani

Geoengineering Research Group, Carleton University, Ottawa, Canada

Abstract

The ultimate shaft capacity of pile foundations in frozen grounds has long been correlated to the long-term shear strength of the surrounding frozen soils using a surficial roughness factor "m". This roughness factor is different for different pile materials (e.g., steel, concrete, and timber), but is often assumed to be constant for any soil type, ground temperature, or stress condition. The current study evaluates the validity of the proposed roughness factor "m" for steel piles embedded in frozen clay and exposed to different scenarios of ground temperatures and normal stress levels. Interface element tests were utilized to characterize the shear strength of frozen Leda clay and the adfreeze strength of the pile-frozen clay interface and to investigate the proposed roughness factor "m" for steel piles exposed to various temperatures and normal stress conditions. The experiments were carried out in a walk-in temperature-controlled environmental chamber. Roughness factor "m" was found not to be a constant number for a given pile material, but rather to decrease with an increase in the freezing temperature. A frictional factor "n", analogous to roughness factor "m", was also introduced to correlate the frictional resistance of frozen soil to the frictional resistance of the pile-soil interface. A temperature-dependent empirical equation was also proposed for predicting the shaft capacity of steel piles based on the shear strength parameters of the surrounding ice-rich clay soil.

1. Introduction

The performance of pile foundations in frozen grounds has long been evaluated both in the field (e.g., Vialov 1959; Crory 1963; Johnston and Ladanyi 1972; Nixon 1988; Biggar and Sego 1993; Aldaeef and Rayhani 2019a, 2019b) and in the laboratory (e.g., Parameswaran 1978, 1979, 1981, 1987; Sego and Smith 1989; Ladanyi and Theriault 1990; Aldaeef and Rayhani 2017). However, most design procedures were developed based on data collection and interpolations with limited comprehensive studies on the performance of pile foundations in various types of frozen soils when exposed to different temperatures and different stress conditions (e.g., Nixon and McRoberts 1976; Nixon 1978; Morgenstern et al. 1980; Weaver and Morgenstern 1981).

Frozen soil is a multiphase system of ice, unfrozen water, air, and soil particles. Thus, the mechanical response of pile foundations in frozen grounds could be more complex than that in unfrozen grounds. Frozen soil, in general, exhibits viscoplastic strength and deformation behaviors due to the presence of an ice matrix, showing time-dependent mechanical responses. The strength of frozen soils is the result of the cohesion of the ice matrix (known also as cementation bonds) and the frictional resistance generated between the solid particles (Williams & Smith

Please cite this article as: A. A. Aldaeef and M. T. Rayhani, Interface shear strength characteristics of steel piles in frozen clay under varying exposure temperature, Soils and Foundations, https://doi.org/10.1016/j.sandf.2019.11.003

1991). However, the strength of frozen soils cannot simply be represented by the sum of the strengths exerted by the crystalline ice and soil grains (Ting 1981).

Upon freezing, fine-grained soil is expected to preserve a considerable amount of unfrozen water content even at relatively low temperatures. Therefore, besides the thermodynamic condition of the ice-water-soil system, ice could be only one aspect that requires consideration. A varying freezing temperature can cause major changes in the mechanical behavior of frozen soils due to the proportional changes in the quantity of the unfrozen water content. Even with a small amount of unfrozen water content, such as in ice-poor frozen sand, a change in temperature can still cause significant changes in the strength behavior because of the considerable effect of the water phase change from solid to liquid, as reported by Williams & Smith (1991). This was experimentally proven by many researchers, including Aldaeef and Rayhani (2017), who observed an adfreeze bond reduction of approximately 90% after the exposure temperature increased from $-1.5\,°C$ to $0\,°C$. The significant role of the unfrozen water content has been attributed to its existence at the points of contact between the soil particles as well as at the pile-soil interface, substantially influencing the ice bonding concentration (Williams & Smith 1991).

Parameswaran (1978) reported that the ultimate bearing capacity of piles depends mainly on the shaft resistance along the permanently frozen depth. The strength gained from end bearing could be negligible for piles installed in ice-rich soils and may only be significant if the piles are installed in ice-poor frozen soils such as bedrock or granular soils (Crory 1963). The US Army/Air Force (1967) suggested that the end-bearing capacity could be ignored in design considerations for piles with base diameters smaller than 150 mm regardless of the soil type. This was attributed to the greater movement that is required to mobilize the end bearing compared to the much smaller movement needed to overcome the adfreeze bond along the pile shaft.

The principle of the design criteria for pile foundations in frozen soils was initially based on the allowable adfreeze strength obtained from the ultimate adfreeze strength of the pile-soil interface (e.g., Vialov (1959), Crory and Reed (1965), Penner (1970, 1974), Penner and Irwin (1969), Penner and Gold (1971), and Dalmatov et al. (1973)). Johnston and Ladanyi (1972), in contrast, determined the allowable load capacity based on the adfreeze strength that would cause an allowable displacement (or creep) rate over the lifetime of structures to accommodate for the time-dependent behavior of frozen soils. Other researchers, including Nixon and McRoberts (1976), Morgenstern et al. (1980), and Weaver and Morgenstern (1981), suggested checking both the adfreeze strengths and the design based on the smaller values amongst them.

An empirical equation proposed by Vialov (1959) was one of the earliest approaches for estimating the long-term adfreeze strength of piles in frozen grounds as a function of the ground temperature. The equation was derived based on experimental data collected from full-scale loading tests on timber piles hand-driven into pre-steamed holes in silty sandy loam and argillaceous loam, as follows:

$$\tau_{al} = \sqrt{1.65\,\theta\,(°C)} - 0.3 \tag{1}$$

where τ_{al} is the long-term adfreeze strength (kgf/cm^2) and θ is the positive value of the temperature below the freezing point (°C). Later, in 1963, Crory (1963) conducted a series of full-scale loading tests on 200-mm-diameter steel pipe piles installed in predrilled frozen silty sand and shaft-grouted with silt-water slurry under an average ground temperature of $-4°C$ to $0\,°C$. His results agree very well with the results reported by Aldaeef and Rayhani (2017) for the ultimate adfreeze strength of steel piles in ice-poor soils using interface element tests. The results from both studies may be expressed in the following form:

$$\tau_{ul} = 0.098T(°C) + 0.0581 \tag{2}$$

where τ_{ul} is the ultimate adfreeze strength (MPa) and T is the positive value of the freezing temperature (°C). Parameswaran (1978) tested model piles made from different materials in frozen sand at $-6°C$ and reported that the peak adfreeze strength was at its maximum for wood piles, followed by concrete piles and then steel and coated piles. Weaver and Morgenstern (1981) correlated the long-term adfreeze strength (τ_{al}) to the long-term shear strength of frozen soil (τ_{lt}) using a roughness factor "m" that characterizes the pile surface and other pile surficial variables such as impurities. The long-term adfreeze strength is expressed by the following formula:

$$\tau_{al} = m\tau_{lt} \tag{3}$$

The long-term shear strength of frozen soils (τ_{lt}) has often been expressed using the Mohr-Coulomb failure criterion, as follows:

$$\tau_{lt} = C_{lt} + \sigma_n \tan \varnothing_{lt} \tag{4}$$

where C_{lt} and $\varnothing_{lt}$ are the long-term strength parameters of frozen soils and σ_n is the normal stress acting on the shear plane. Weaver and Morgenstern (1981) stated that, in frozen grounds, the normal stress on the shear plane is typically less than 100 kPa. This may make the contribution of the frictional component to the total pile strength insignificant; and thus, it may be disregarded. Therefore, the long-term adfreeze strength was reduced to

$$\tau_{al} = mC_{lt} \tag{5}$$

Roughness factor "m" was first extrapolated by Weaver and Morgenstern (1981) when data on the shear strengths of frozen soils were compared to data on the pile-soil adfreeze strengths. A roughness factor of 0.7 was suggested for uncreosoted timber piles based on the ratio between the adfreeze strength of timber piles in ice to the long-term cohesion of ice obtained from the field and experimental data of Voitkovskii (1960) and Vialov (1959). A roughness factor of 0.6 was inferred for steel and concrete piles based on data from field experiments conducted by Johnston and

Ladanyi (1972) and Crory (1963). Weaver and Morgenstern (1981) stated that the long-term adfreeze strengths of steel and concrete piles in the data they used were not well defined; however, 0.6 represented the lower boundary and could still be acceptable for conservative pile designs. Ladanyi and Theriault (1990) evaluated the soil-metal adfreeze bond at −2°C and reported that the long-term shaft resistance of piles in frozen grounds does not solely depend on the long-term adfreeze, but also on the long-term friction angle at the interface and on the total normal stress. Therefore, they improved Weaver and Morgenstern's (1981) equation by adding the contribution of the long-term friction angle of frozen soil and proposed the following formula:

$$\tau_{al} = mC_{lt} + \sigma_{n\text{total}} \tan \varnothing_{lt} \qquad (6)$$

Interestingly, the experimental results of Ladanyi and Theriault (1990) showed that the frictional resistance was not only dependent on the normal stress, but also on the roughness factor. For a steel-frozen sand interface, the roughness factor increased from 0.1 to 0.3 when the normal stress was increased from 100 kPa to 1100 kPa, but it never reached the value of 0.6 that had been suggested by Weaver and Morgenstern (1981). Although Ladanyi and Theriault (1990) were not confident of using their short-term study to validate the roughness factor, and they suggested more investigations, continuing to use the constant roughness factors in the way that was proposed by Weaver and Morgenstern (1981) became questionable.

There are some uncertainties associated with the suggested roughness factors as they were extrapolated from very limited field and laboratory data that lacked important information on soils and piles under certain conditions. The data used by Johnston and Ladanyi (1972) and Crory (1963), for example, were obtained from their field studies on the adfreeze strength of steel rods and steel pipe piles, respectively, with no record of experiments on concrete piles. It is not clearly shown that the adfreeze strength of piles and the shear strengths of frozen soils were obtained under identical conditions (i.e., pile material, soil type, stress history, and thermal boundary) that would allow for reliable comparisons and accurate estimations of the roughness factors. The roughness factor for a steel pile in frozen sand, for instance, could be different from that in frozen clay or silt. It could also be different for two identical steel piles embedded in the same type of soil, but exposed to different ground temperatures or installed at different depths. The soil to soil interaction behavior may be different from pile to soil interaction characteristics which may result in different responses at different exposure conditions, thus leading to different roughness factors.

The current study summarizes the results of experimental programs dedicated to evaluating the impact of thermal exposure on the shear strengths of ice-rich soils and the shaft resistance of steel piles in ice-rich soils. Several direct shear tests were conducted inside an environmental chamber to measure the cohesion and friction angle of frozen soil, the steel-soil adhesion, and the steel-soil friction angle at different temperatures and normal stress levels. Accordingly, roughness factor "m" was reevaluated under different thermal boundaries and loading conditions. Moreover, the paper discusses the contribution of frictional resistance to the shaft capacity of steel piles in ice-rich soils.

2. Test materials

2.1. Soil material

A marine soil, known as Leda clay, was used in this experiment to represent the ice-rich frozen materials. The

Fig. 1. Soil sampling at Navan Landfill site in Ottawa.

Table 1
Physical and hydraulic properties of the test soil.

Characteristic	USCS	$w_{i_{ave}}$(%)	LL (%)	PI	$\rho_{b_{ave}}$(Mg/m^3)	% clay	Activity	k (m/s)
Physical & hydraulic properties	CH	75	51	24	1.624	71	0.34	5.9E-10

Table 2
Chemical and mineralogical properties of the test soil.

Characteristic	Sodium (mg/kg)	Potassium (mg/l)	Calcium (mg/l)	Magnesium (mg/l)	(CEC)* meq/100 g	Illite	Chlorite	Kaolinite
Chemicals and minerals	1700	15	83	40	18	83	6	11

* Cation exchange capacity.

clay soil was sampled intact from the Navan Landfill site in Ottawa, Ontario. The sampling was conducted using 200-liter steel barrels that were carefully pushed into the natural Leda clay using a backhoe (Fig. 1). Before the sampling, the inside surface of the barrels was coated with a thin layer of wax. After the sampling, the top of each clay sample was trimmed, waxed, and sealed with airtight plastic sheets followed by a steel lid to ensure the maintenance of the natural water content of the collected samples.

The basic geotechnical properties of Leda clay, including the particle size distribution, the Atterberg limits, the bulk density, and the natural water content, were examined (Table 1). The particle size distribution and the clay content of the Leda clay were determined using a sieve analysis and hydrometer tests in accordance with ASTM D422-63. The liquid limit of the soil was 51%, while the plasticity index was 24% based on the Atterberg limit test results (ASTM D4318-10). The average bulk density and water content of the test samples were 1.624 Mg/m^3 and 75%, respectively. The hydraulic conductivity of the clay sample was also measured according to the Falling Heading testing technique and using a Rigid-Wall mold (ASTM D5856-95, 2007) equipped with a rubber membrane to minimize the side-wall leakage (Table 1).

A chemical analysis was also performed on the extracted pore water obtained by squeezing the soil samples under very high pressure. The cation concentrations, including potassium, calcium, and magnesium ions, were determined in the pore water (mg/l), while the sodium concentration was measured based on the acid extractable sodium ions (mg/kg). The cation exchange capacity (CEC) was also determined and the results are presented in Table 2. A random X-ray powder diffraction analysis was carried out to determine the mineralogical composition of the Leda clay. A semi-quantitative analysis was conducted on the X-ray results to measure the clay mineral components. The most abundant clay mineral found in this soil was illite, comprising 83%. The remaining mineral portion comprised kaolinite and chlorite with amounts of 11% and 6%, respectively. The results indicated no evidence of any expandable clay minerals (here defined as vermiculite, montmorillonite, or interlayered illite/ smectite) in the test soil (Table 2).

2.2. Characteristics of the model pile material

Structural steel specimens were used in this study to represent the pile material for the pile-soil interface tests. Steel is a common pile material used in cold regions for manufacturing steel piles in several geometries, including pipe piles, H-section piles, and helical piers. For relatively warm permafrost, open-ended steel-pipe and H-steel piles can be driven deeply enough into permafrost to develop a sufficient adfreeze bond and to provide a high bearing capacity. In cold permafrost, closed-ended pipe piles may be installed in oversized predrilled holes and backfilled with sand-water slurry or grouted with concrete. Pile installation in pre-thawed permafrost, using steam or hot water, is widely used for H-piles and pipe piles (Kitze 1957).

In this experiment, a steel plate, 90 mm by 90 mm, was used to simulate the shaft surface of a typical steel pile. It was machined to couple with the upper half of the direct shear box and to provide a steel-soil interface area of 60 mm by 60 mm. The total and average surface roughness values for this particular type of steel were measured as 9.7 μm and 11.3 μm, respectively. The steel plate was equipped with a copper-constantan thermocouple reader inserted in a 1-mm diameter hole predrilled underneath the upper surface of the plate. A 1-mm diameter window was made in the middle of the steel plate such that the sensing end of the thermocouple reader would be in contact with the soil sample in order to track the temperature changes at the steel-soil interface (Fig. 2b).

3. Test equipment

The roughness factor represents the ratio between the pile-soil adhesion strength and the cohesion strength of frozen soils. Obtaining this factor, however, would require using a representative cold environment and a suitable testing technique. Thus, this experimental investigation was carried out in a walk-in environmental chamber that enabled cooling to the desired freezing temperature through an automatic temperature control system. Although the temperature in the environmental chamber fluctuated ±0.5 °C, the temperature fluctuation within the

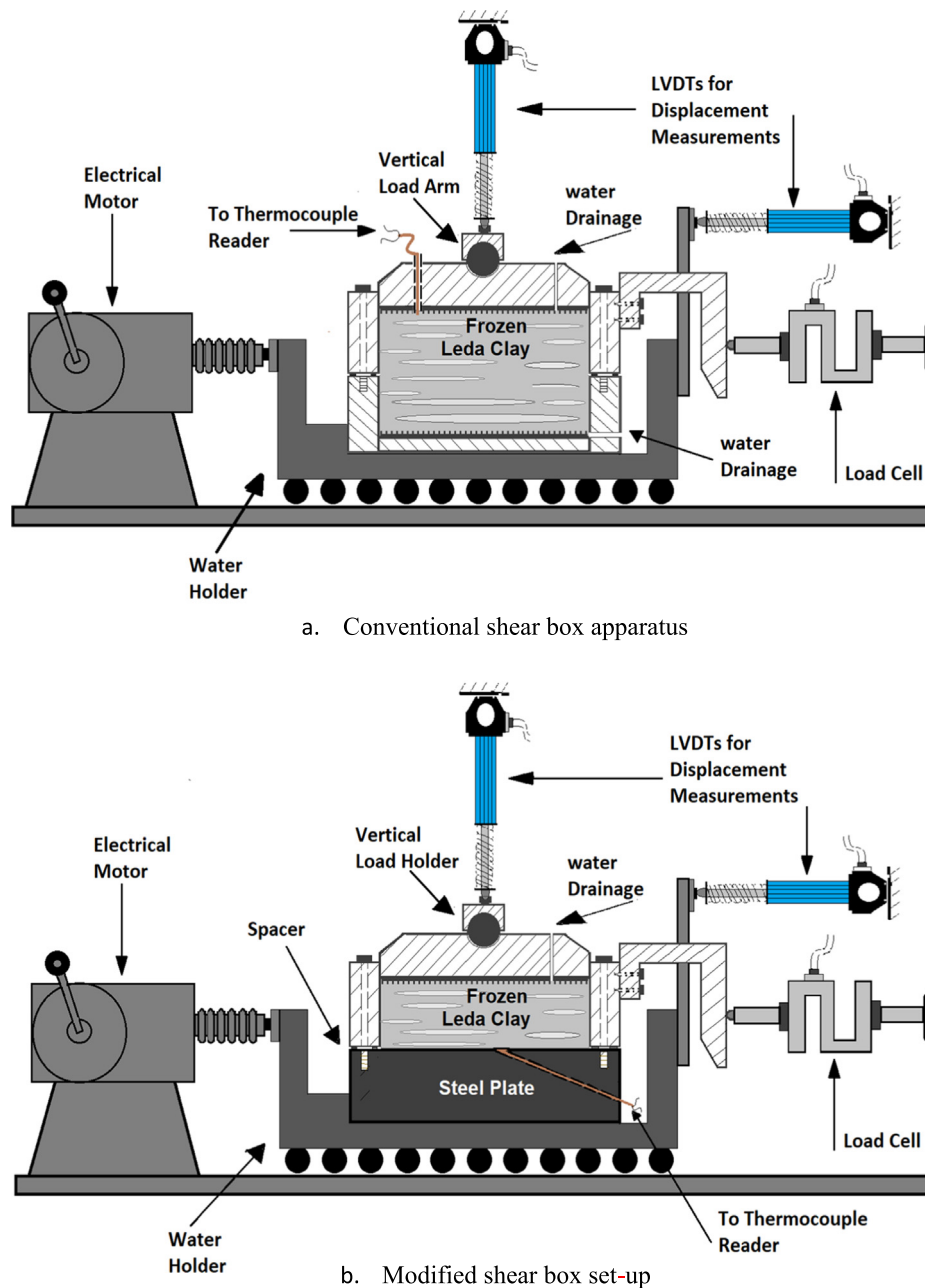a. Conventional shear box apparatus

b. Modified shear box set-up

Fig. 2. Conventional and modified shear box assemblies for shear strength testing.

test samples was ±0.1 °C as tracked by the thermocouple reader.

For evaluating the adfreeze shear strength and the shear strength of frozen clay, a modified direct shear test apparatus was employed in accordance with ASTM D3080/D3080M-11 and ASTM D5321-12. The apparatus consists of conventional and modified shear boxes designed to mount on a shear-rate-controlled testing frame (Fig. 2a and b). The conventional shear box, which was used to test the shear strength parameters of the frozen clay, consists of two attachable hollow square parts designed to confine the test sample within the hollow space and machined to facilitate shearing along a predefined horizontal plane. In con-

trast, a modified shear box was used to test the steel-soil adfreeze shear strength. It consists of a lower solid square steel plate machined to couple with the upper hollow square part of the shear box such that a steel-soil interface element is produced to simulate the pile set-up in the field and to facilitate shearing along the line of the interface.

The direct shear test apparatus was placed inside the walk-in environmental chamber to enable shear testing at various temperatures below the freezing point. The testing mechanism of the apparatus depends on imposing a constant horizontal shear velocity on the test sample while continually recording the shear force, the horizontal shear displacements, and the vertical displacements. The dis-

placements were measured by Linear Variable Differential Transducers (LVDTs) to an accuracy of 0.001 mm. The desired normal stress was applied using a dead load subjected vertically to the top of the soil sample through a steel-bearing arm. The test data were recorded at a frequency of one data point per second using a data acquisition system and plotted in-real time on a LabVIEW platform.

4. Sample preparation

All the test samples were obtained from Leda clay soil in 200-liter steel barrels. A Shelby tube sampler, with an inner diameter of 101.6 mm, was used for the soil coring from the barrel. The soil was then extracted from the Shelby tube using a mechanical extruder and cut into two different heights, namely, 60 mm for the frozen soil testing and 30 mm for the steel-soil interface testing. For the frozen soil testing, the 60 mm-high cylindrical specimens were trimmed to a square shape of 62 mm × 62 mm. The upper hollow square part of the shear box was oiled and gently pushed through the clay specimen, followed by the lower part, until the soil reached the base of the lower part of the shear box and the two parts of the shear box came into contact with each other. The two parts were then tightened together with steel screws and the top of the clay specimen was trimmed to the final height. A similar procedure was followed for preparing the interface samples where the upper hollow square part of the shear box was oiled and gently pushed through the 30-mm-high clay specimens. The upper part of the shear box, containing the soil specimen, was then placed on top of the steel plate and they were tightened together with two steel screws. The soil specimen in the upper part of the shear box was then gently pushed back against the steel plate to ensure full contact between the soil and the steel plate. The top of the soil specimen was then trimmed to the final height. The final dimensions of the clay specimens used for the shear strength testing of the frozen clay were 60 mm by 60 mm by 50 mm compared to the specimen's dimensions of 60 mm by 60 mm by 25 mm used for the adfreeze strength testing of the steel-soil interface. The initial bulk density, initial gravimetric water content, and ultimate shear strength of each test sample are presented in Table 3.

5. Consolidation and freezing process

To evaluate the consolidation behavior of the test soil, a T5 tensiometer was inserted at the base of the direct shear box such that the ceramic tip of the tensiometer would penetrate the bottom of the clay specimen. The tensiometer enabled the measurement of the excess pore water pressure (PWP), while an LVDT was used to measure the consolidation settlement all corresponding to the applied normal stresses. This test set-up provided information on the time needed for the PWP dissipation and consolidation settlement processes under the test normal stresses, thus ensuring the achievement of effective consolidation pressure before starting the process of freezing. Fig. 3 shows a sample of the excess PWP history and the consolidation settlement for a specimen exposed to a normal stress of 400 kPa.

As the normal stress of 400 kPa was applied to the test sample, the excess PWP, and hence, the consolidation displacement, respectively progressed. The excess PWP reached a maximum value of around 92 kPa shortly after the application of normal stress and then started to decline over time to achieve complete dissipation after 100 min of the load onset. A similar period of time for the excess PWP dissipation in the same type of soil was reported by McQueen et al. (2015) from Cone Penetration test results. The consolidation settlement, on the other hand, showed a major increase as the normal stress was applied and the excess PWP tended to dissipate with the progress of the consolidation. As the excess PWP completely dissipated, the rate of consolidation settlement significantly decreased, recording a strain rate of 0.002%/min at the end of test. This indicates that the sample may have completed the consolidation settlement stage and entered into the creep settlement stage. To compare the excess PWP and displacement histories with the temperature history, the change in temperature over the time was plotted in Fig. 3. The temperature in the cold room was cooled down to 0.0 °C and then changed to the freezing test temperature which, in this example, was −10.0 °C. Similar cooling and freezing processes were followed for the test specimens used in the shear testing under various freezing test temperatures. The results showed that the excess PWP had fully dissipated well before the temperature reached the freezing point. Indeed, the temperature within the test sample dropped from +22.0 °C to +8.0 °C for the first 100 min over which a complete consolidation was observed. Beyond this point, 170 min were needed to cool the test sample to +0.2 °C, followed by 330 min that were required to freeze the test sample to −10.0 °C. These results confirm that the test samples will be fully consolidated during the cooling time period and well before the freezing process is begun. Therefore, this process has been adopted for preparing the test samples for shear testing. The peaks of the pore water pressures and consolidation settlements were smaller under lower normal stresses; thus, shorter times were respectively observed for the PWP dissipation and consolidation settlement. Due to the limitations associated with the operational range in temperature of the T5 tensiometer sensor, the test set-up for measuring the PWP dissipation and consolidation settlement was terminated when the sample temperature reached +1.0 °C and before entering the freezing stage to prevent any damage to the sensor. Therefore, only the temperature measurements over time were continued during the freezing process. The volumetric water content (VWC) was also measured from a dummy soil sample parallel to the PWP measurement to ensure the frost-free condition at +1.0 °C. The results showed that the VWC remained constant and was equal to 0.68 m^3/m^3. This ensured that the water

Table 3
Summary of initial bulk density and initial gravimetric water content along with ultimate frozen shear strength at various test conditions.

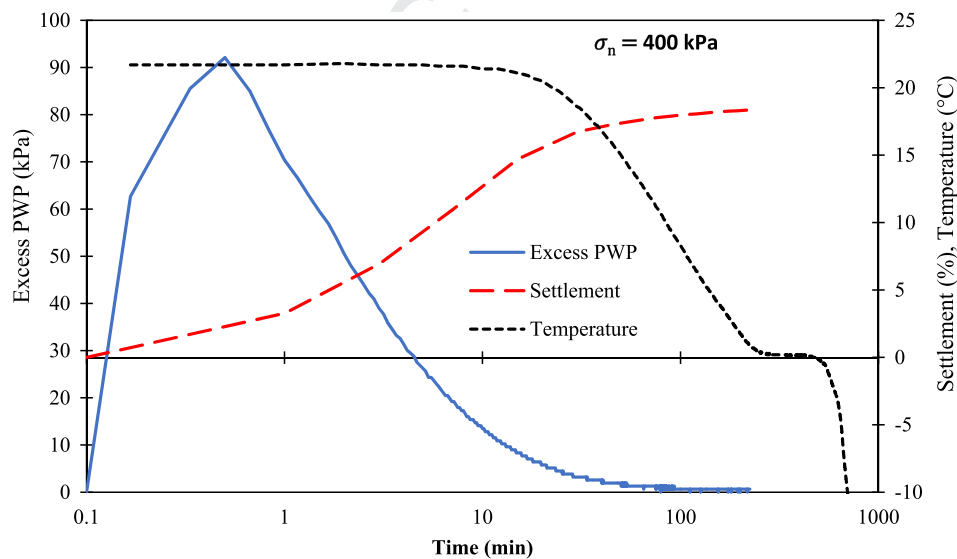| T (°C)	σ_n(MPa)	Clay soil specimens			Soil-steel interface specimens		
		ρ_{bi}(Mg/m³)	w_i(%)	τ_{ult}(MPa)	ρ_{bi}(Mg/m³)	w_i(%)	τ_{ult}(MPa)
−10	0.025	1.621	76.3	1.97	1.634	75.8	1.90
	0.05	1.625	75.2	2.04	1.628	74.0	1.927
	0.10	1.619	76.8	2.10	1.628	76.5	2.08
	0.20	–	–	–	1.624	74.2	2.36
	0.40	1.622	74.9	2.40	–	–	–
−7	0.025	–	–	–	1.627	77.0	1.356
	0.05	–	–	–	1.622	75.1	1.45
	0.10	1.626	75.1	1.561	1.617	76.9	1.50
	0.20	1.624	74.0	1.60	1.625	73.8	1.80
	0.40	1.618	76.5	1.791	–	–	–
−4	0.025	1.631	74.8	1.10	1.623	76.5	0.833
	0.05	–	–	–	1.629	74.4	0.90
	0.10	1.624	73.3	1.172	1.624	77.1	0.952
	0.20	1.619	76.8	1.278	1.631	75.9	1.181
	0.40	1.627	75.9	1.30	–	–	–
−2	0.025	1.617	76.1	0.71	1.632	75.1	0.556
	0.05	–	–	–	–	–	–
	0.10	1.622	73.6	0.833	1.629	73.8	0.611
	0.20	1.621	77.3	0.833	1.622	76.2	0.736
	0.40	1.625	75.4	0.92	–	–	–
−1	0.025	1.628	74.2	0.653	1.620	74.8	0.436
	0.05	1.624	74.0	0.70	–	–	–
	0.10	1.632	74.7	0.683	1.627	75.0	0.522
	0.20	1.621	74.9	0.744	1.631	75.9	0.597
	0.40	–	–	–	–	–	–
0	0.025	1.626	73.1	0.40	1.616	76.4	0.236
	0.05	–	–	–	–	–	–
	0.10	1.627	77.6	0.431	1.627	75.2	0.264
	0.20	1.627	76.3	0.472	1.623	75.9	0.355
	0.40	–	–	–	–	–	–

Fig. 3. Excess pore water pressure history and consolidation settlement of specimen under normal stress of 400 kPa during cooling along with temperature history for cooling and freezing to −10.0 °C.

potential was not influenced by the cooling process up to +1.0 °C at which time the PWP measurement was terminated.

For the shear test, the soil specimen was mounted on the direct shear test apparatus inside the environmental chamber. Immediately afterwards, the desired normal stress was

applied. The temperature was then cooled down to close to the freezing point over a period of 270 min, as shown in Fig. 3, allowing for consolidation and PWP dissipation. Subsequently, the freezing process was started and continued until reaching the desired test temperature. The purpose of maintaining the normal stress during freezing was to produce uniform element test specimens by minimizing the formation of ice lenses, and thus, reducing the inhomogeneity (Wang et al. 2017). The absence of confining pressure during freezing, particularly under a slow rate, could lead to the formation of small ice lenses that may reduce the uniformity of the test specimens (Viggiani et al. 2015; Wang et al. 2017).

Although one-dimensional freezing action is expected to happen in the field, simulating this field condition in the present experiment was challenging. The main difficulties were associated with the limited space around the test sample and the standard instrumentation fabrications of the test apparatus that prevented the adoption of a reliable measure for imposing 1-D freezing action. Given these limitations, the test samples in this experiment were exposed to freezing from all around. Nevertheless, the soil in the field may still experience freeze-back from more than one direction post-pile installation. Two-way freezing action could be enhanced by the superior thermal conductivity of the steel pile at one side and the presence of frozen soil in the vicinity of the pile on the other side. Therefore, this experiment is believed to have captured many aspects of pile foundations in the field.

6. Test procedure

6.1. Shear strength testing

A total of 68 shear tests were conducted in this study to evaluate the shear strength of frozen clay and the adfreeze strength of the steel-clay interface. Out of the 68 tests, 22 tests were used for a test-retest reliability assessment and to ensure test repeatability. All the tests were conducted following similar procedures. After placing the test sample inside the environmental chamber, it was left for 24 hrs to acquire thermal and volumetric equilibrium under the desired temperature and normal stress. After 24 hrs, the two steel screws were removed to allow for the two parts of the shear box to move along the line of the interface. The shear load was subsequently subjected to the lower part of the shear box/steel plate, while the upper part of the shear box was restrained by the load cell for measuring the shear resistance. The shear load was applied at a constant shear rate of 0.011 mm/min (i.e., 16.3 mm/day). This shear rate was adopted from a similar study performed by Ladanyi and Theriault (1990) on ice-poor frozen sand. Using similar shear rates to those reported in literature and applied to different test materials may be useful for discovering the differences in the shear behaviors of various types of frozen grounds. The shear tests were conducted at various temperatures, including $-10\,°C$, $-7\,°C$, $-4\,°C$, $-2\,°C$, $-1.0\,°C$, and $0\,°C$. At each temperature, the peak shear strengths and peak interface adfreeze strengths were determined under various normal stresses, including 25 kPa, 50 kPa, 100 kPa, 200 kPa, and 400 kPa.

7. Results

7.1. Shear strength of frozen Leda clay

Stress-displacement curves for the frozen Leda clay samples tested at various temperatures and under various normal stresses are presented in Fig. 4. Peak strengths were typically observed at shear displacements ranging from 0.36 mm to 2.4 mm and representing a shear strain range of 0.6%–4.0%, respectively. The variation in shear displacement at the peak was mostly associated with the test temperature where the soil samples tested at higher freezing temperatures failed at lower shear displacements. As the test temperature was decreased, however, the shear displacement at failure increased. Most of the shear tests were continued after the failure up to 10% strain (6-mm displacement) in an attempt to characterize the residual shear strength.

Frozen soils tested at temperatures lower than $-4.0\,°C$ always showed a brittle failure mode demonstrated by the significant strength losses recorded right after the peaks. As the test temperature rose to higher than $-4.0\,°C$, however, the samples started failing in a plastic manner, exhibiting less catastrophic failure with relatively smaller differences between the peak and the residual strengths.

In this experiment, the temperature was shown to have a substantial effect on the strength behavior of frozen clay. The soil tested at $-10\,°C$ under a normal stress of 25 kPa, for example, showed a peak strength of around 2 MPa. However, its strength under the same normal stress but at the freezing point temperature, underwent a significant reduction, demonstrating an ultimate capacity of around 0.45 MPa. This thermal change decreased the shear strength of the frozen clay by almost 4.5 times, causing a reduction in strength of 78%. The loss in strength corresponding to the applied warming action could be attributed to the decrease in the adfreeze bond due to the reduction in the ice content and the increase in the unfrozen water content.

7.2. Shear strength of steel-soil interface

The steel-soil interface testing program was aimed at studying the strength behavior of pile foundations in frozen clay. The results from this experiment followed a similar pattern to that exhibited by the frozen clay with minor differences (Fig. 5). The interface peak strengths, for instance, were usually measured at slightly smaller shear displacements compared to the frozen soil tests recording displacement values ranging from 0.18 mm to 2.1 mm. As with frozen clay, a higher displacement was recorded at the peak for the interface tests conducted at lower freezing tempera-
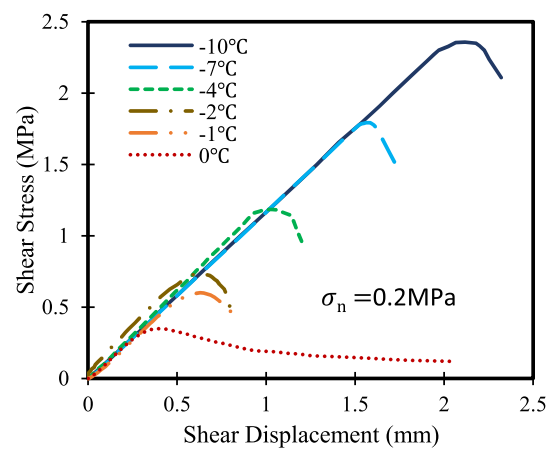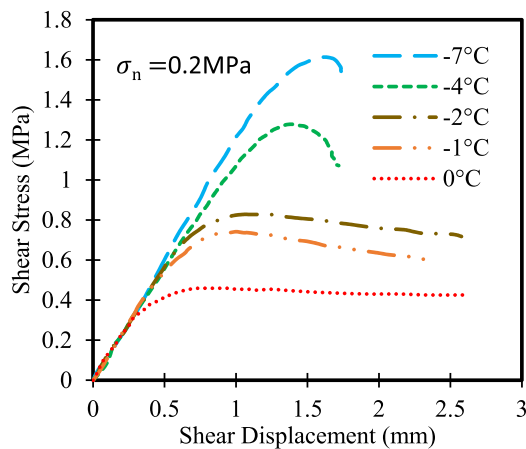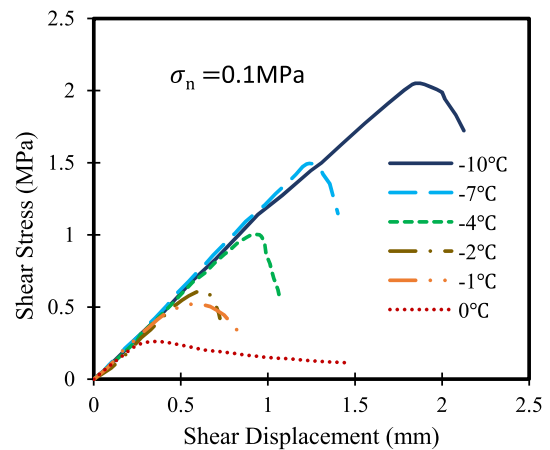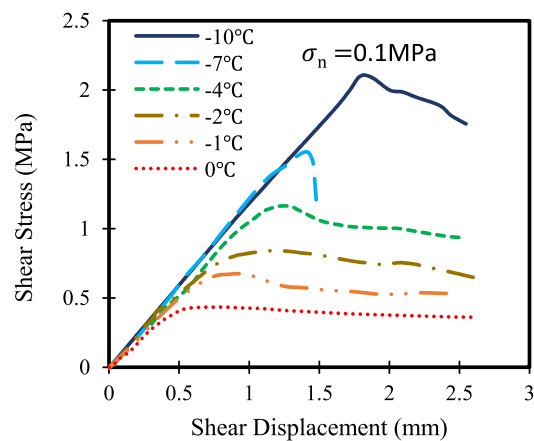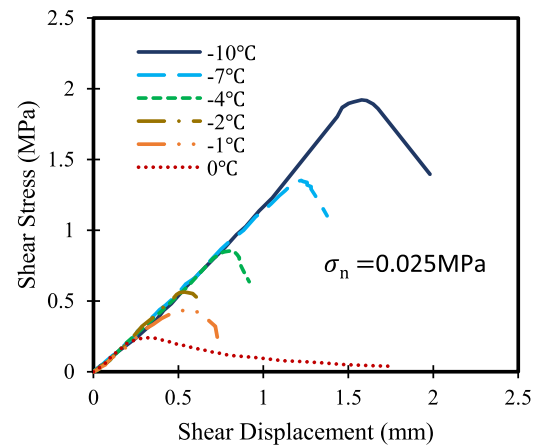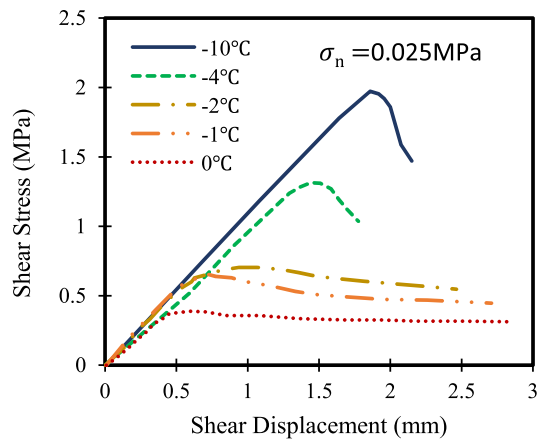
Fig. 4. Stress-displacement curves for frozen clay at different temperatures and normal stresses.

Fig. 5. Stress-displacement curves for steel-soil interface at different temperatures and normal stresses.

tures. This often would signify a higher ice bond that needed greater energy to be overcome. Brittle behavior dominated most of the interface tests and was more pronounced than the behavior witnessed during the frozen clay testing. Subsequently, the interface samples showed immense reductions in strength right after the peak and demonstrated very small residual strengths. The interface tests conducted at 0 °C, however, showed less intensive brittle failure and recorded a smooth transition toward plastic behavior.

Freezing temperatures often show a proportional correlation to the ice content and ice bonding concentration, and thus, to the peak strength too. This could be the reason for the higher peak interface strengths witnessed at lower freezing temperatures. At a normal stress of 25 kPa and a test temperature of -10 °C, the interface peak strength

was around 1.9 MPa. However, the strength under a similar normal stress, but at a temperature of 0 °C, underwent a significant reduction, demonstrating an ultimate capacity of around 0.25 MPa. This thermal change led to the weakening of the shear strength of the steel-soil interface by more than 7.5 times, causing a reduction in strength of almost 85%. Indeed, this highlights the significant impact of thermal changes on the ultimate bearing capacity of steel piles in frozen grounds. Although such a dramatic increase in temperature may not be encountered, especially when considering the macroscale level (i.e., effects of global warming), it may occur in the microscale level for different reasons, including improper thermal insulation measures and/or induced warming due to improper pile installation techniques.

8. Analysis and discussion

The results obtained from this study were used to develop a better understanding of the performance of pile foundations in frozen ice-rich soils. One main goal of the study was to evaluate the possible variation in the roughness factor corresponding to thermal changes. Normal stress acting on the pile shaft could be another important aspect to address in this study. In particular, the attempts could be toward quantifying the contribution of frictional resistance to the ultimate shaft capacity of the piles by bringing together the results of this study along with the hypotheses available in literature on the frictional resistance and lateral earth pressure in frozen soils. A correlation between ground temperature and the ultimate shaft capacity of pile foundations can be established and introduced in forms of graphical and/or empirical equations.

8.1. Effect of ground temperature on the surficial roughness factor "m" of steel piles in frozen clay

Regardless of the ground temperature and soil type, a constant roughness factor of 0.6 has long been used to correlate the adfreeze strength of steel and concrete piles to the long-term shear strength of the surrounding frozen soil. In this section, efforts are made to evaluate the suitability of this assumption by comparing the peak shear strength of frozen Leda clay with the peak adfreeze strength of steel-clay interfaces at various temperatures. Using the Mohr-Coulomb failure criterion, the peak strengths versus normal stresses at different freezing temperatures were plotted for frozen clay and steel-frozen clay interfaces (Fig. 6). Table 4 presents the strength parameters for the frozen clay soil and the pile-soil interface tests.

For each test temperature, the intercept of the failure envelopes of the frozen clay samples and the steel-pile interface elements with the vertical axis defines the cohesive and adhesive strengths, respectively. The cohesive strength of frozen clay was always higher than the adfreeze strength of the pile-soil interface. This could be attributed to the one-way drainage path formed within the pile-soil interface element. The one-way drainage path is enhanced by the existence of the impermeable steel plate which, in practice, represents the pile foundation.

The one-way drainage path may have delayed the movement of unfrozen water away from the shear plane during consolidation and refreezing. As a result, this may have contributed to a higher inter-particle unfrozen water content compared to the case of clay samples for which a two-way drainage path exists.

The accumulation of the unfrozen water content at the pile shaft would, therefore, lessen the ultimate water potential (cryosuction), and subsequently, decrease the ice bonding at the pile shaft. The combination of the soil to soil cohesion and the ice bonding exerted within the frozen clay, compared to the ice bonding alone at the pile-soil interface, could be another contributing factor that resulted in the greater cohesive strength of the frozen soil compared to that of the pile-soil adhesion.

Both the cohesive and the adhesive strengths experienced dramatic reductions as the exposure temperature increased toward the freezing point. This is possibly due to the decrease in ice content and the increase in unfrozen water content as the temperature increased. The adhesive strength, however, underwent more pronounced degradation compared to the cohesive strength of the frozen soil at any given temperature. Once again, this may be attributed to the one-way drainage effects which contributed to the greater accumulation of unfrozen water as the temperature increased. This has therefore resulted in the lowering of the roughness factor to its minimum value of 0.54 when the temperature reached the freezing point. The correlation between the roughness factor and the positive values of the freezing temperatures, plus the unity (T + 1) of the ice-rich soil, was established as presented in Fig. 7. Expressing the freezing temperature in (T + 1) form enabled the power law trend line fitting parameters to be obtained for the experimental data. This mathematical technique was first used by Vialov (1965) and later adopted by Nixon & McRoberts (1976) for correlating the creep parameters of frozen soils to freezing temperatures.

Theoretically, the roughness factor may not be considered constant based on this graphical demonstration, but rather varies exponentially from 0.54 to 0.91, corresponding to a decrease in ground temperature from 0 °C to −10 °C, respectively. Practically speaking, however, the assumption of using a constant value of 0.6 may still be valid and considered conservative as long as the ground temperature is lower than −1°C. For frozen ice-rich soils exposed to higher ground temperatures, the roughness factor cannot be more than 0.5. For a more precise estimation, however, the adhesive strength of steel piles in frozen ice-rich soils could be expressed as a function of the temperature and the cohesive strength of frozen clay using the following equation:

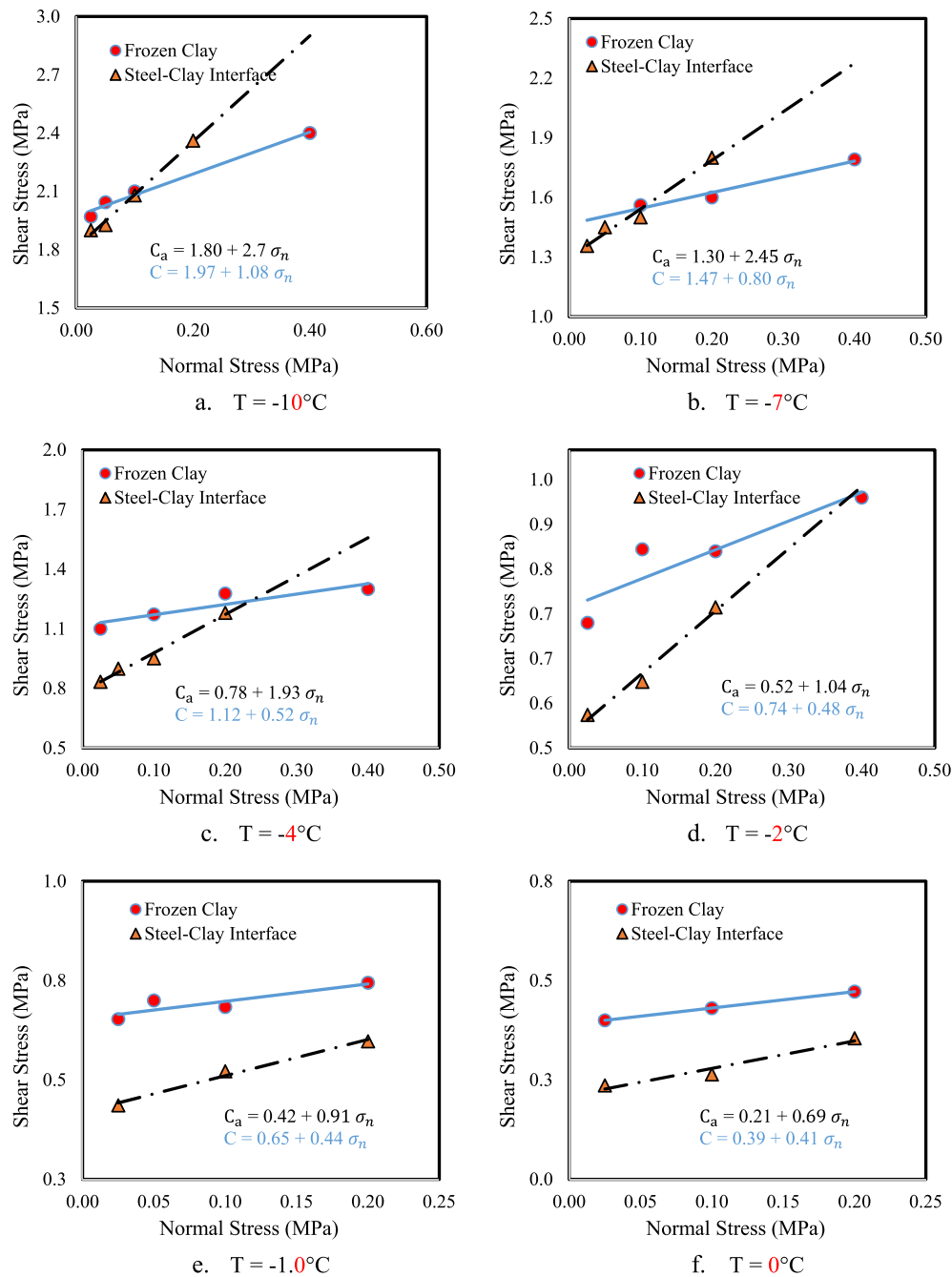$$C_a = 0.54(T + 1)^{0.215}C \tag{7}$$

Fig. 6. Mohr-Coulomb envelopes for frozen clay and steel-soil interface at various freezing temperatures.

Table 4
Strength parameters, roughness factor, and frictional factor at different freezing temperatures.

T °C	Clay-clay interface		Steel-soil interface		m, $\left(\frac{C_a}{C}\right)$	n, $\left(\frac{\tan\delta}{\tan\varnothing}\right)$
	C(MPa)	tan($\varnothing$)	C_a(MPa)	tan(δ)		
−10.0	1.97	1.08	1.8	2.7	0.91	2.50
−7.0	1.47	0.8	1.3	2.45	0.88	3.06
−4.0	1.12	0.52	0.78	1.93	0.70	3.71
−2.0	0.74	0.48	0.52	1.04	0.70	2.17
−1.0	0.65	0.44	0.42	0.91	0.65	2.07
0.0	0.39	0.41	0.21	0.69	0.54	1.68

Fig. 7. Relationship between roughness factor "m" and ground temperature.

where C and C_a are the cohesive strength of the frozen soil and the adhesive strength of the pile-soil interface element at a frozen ground temperature (T), respectively. The frozen ground temperature is substituted in the equation as a positive degree Celsius value. It is worth mentioning that the cohesive strength was not denoted with a long-term strength symbol because, in this experiment, only short-term strengths were obtained. However, the cohesive and adhesive strengths were normalized to each other with respect to time by roughness factor "m". Thus, this equation is believed to be valid for correlating the cohesive strength of frozen soil to the adhesive strength of the pile-soil interface for both short and long-term scenarios.

8.2. Effects of normal stress on shaft resistance of steel piles in frozen clay

Few attempts were made in the past and reported in literature to measure the normal stresses in frozen soils and to investigate their contribution to the ultimate shear strength of frozen soils and to the ultimate adfreeze strength of the pile-soil interface. For example, Johnson & Buska (1988) reported maximum frost heave forces of 800 kN and 1100 kN subjected to H-piles and steel pipe piles backfilled with silt slurry. The associated adfreeze strengths were reported as 214 kPa and 972 kPa, respectively. The normal stress on the pile shafts was estimated from the limited transverse strain gauge readings and found to be one-third of the adfreeze strength, recording a maximum value of 370 kPa observed on the pipe pile shaft. Similar forces/stresses were recorded over three consecutive winters, i.e., 1983, 1984, and 1985, at relatively shallow depths ranging from 1.4 to 2.2 m from the ground surface (within the active layer).

Practically speaking, the installation of pile foundations in frozen grounds could induce an increase in horizontal stress at any depth along the pile shaft. This happens following the refreezing of the slurry around the piles installed in oversized holes or due to the soil freeze-back occurring after the driving of a pile directly into a pre-thawed frozen ground or a slightly undersized hole. The process of freezing-induced normal stress and the stress distribution around the pile after driving it into a pre-thawed frozen ground is illustrated in Fig. 8.

The frozen ground is first melted to a desired depth using steam or a hot water jet. Shortly afterwards, the pile is driven into the melted soil and usually loaded onto the head to minimize the vertical jacking associated with frost heave during the process of soil freeze-back. The melted soil will start to freeze and may acquire a significant freezing condition within hours to a few days (Johnson & Buska 1988). As the soil is frozen-back, its volume increases due to the phase transformation of water from liquid to ice. The volume growth of the refrozen soil is likely to be restrained by the surrounding frozen boundary, thus enhancing the normal stress around the pile shaft which contributes to greater skin friction. Ladanyi (1988) theoretically showed that the mobilized lateral pressure due to the pile installation in ice-rich soils may relax within 24 hrs, falling to less than 1% of the pre-installation lateral pressure. Nevertheless, a rapid dissipation of the mobilized lateral pressure may not occur in frozen soils because of their extremely low permeability and long consolidation time that could be longer than the service life of the structure. This was shown in Johnson & Buska (1988) where a pile shaft strain associated with freezing-induced normal stress gradually increased from Oct. 1983 to Feb. 1984 and then decreased to zero when the soil melted entirely in May 1984. The dissipation of the freezing-induced normal stress was mainly due to the melting of the seasonally frozen active layer. Given that piles are often driven deeply enough into the permanent frozen ground, the induced normal stress may not relax in a short time. Therefore, including the contribution of the freezing-induced normal stress acting on the pile shaft could be important for the pile design and installation in permeant frozen grounds in terms of accurately estimating the ultimate bearing capacity and frost heave. Although the current experiment may not fully capture the way in which normal stress develops, as shown by the conceptual model given in Fig. 8., it involves the testing of various normal stress scenarios that may be experienced in the field from the overburden pressure and leading to soil/backfill refreezing.

In the current study, and from Fig. 6, the inclination in the Mohr-Coulomb failure envelopes indicates higher strengths for frozen soils and steel-soil interface samples as the normal stress becomes greater. This confirms the contribution of the frictional resistance to the ultimate strength of frozen clay and the shaft resistance of steel piles in frozen clay. The frozen clay showed decreased friction angles ($\varnothing$) with increasing temperatures, recording 45° at −10 °C and around 12° at 0 °C. The steel-soil interface friction (δ), on the other hand, followed a similar pattern, but displayed higher values at any given temperature, exhibiting 70° at −10 °C and around 32° at 0 °C (Fig. 9a).

Frictional resistance is predominantly due to the interlocking force of the soil particles which increases with
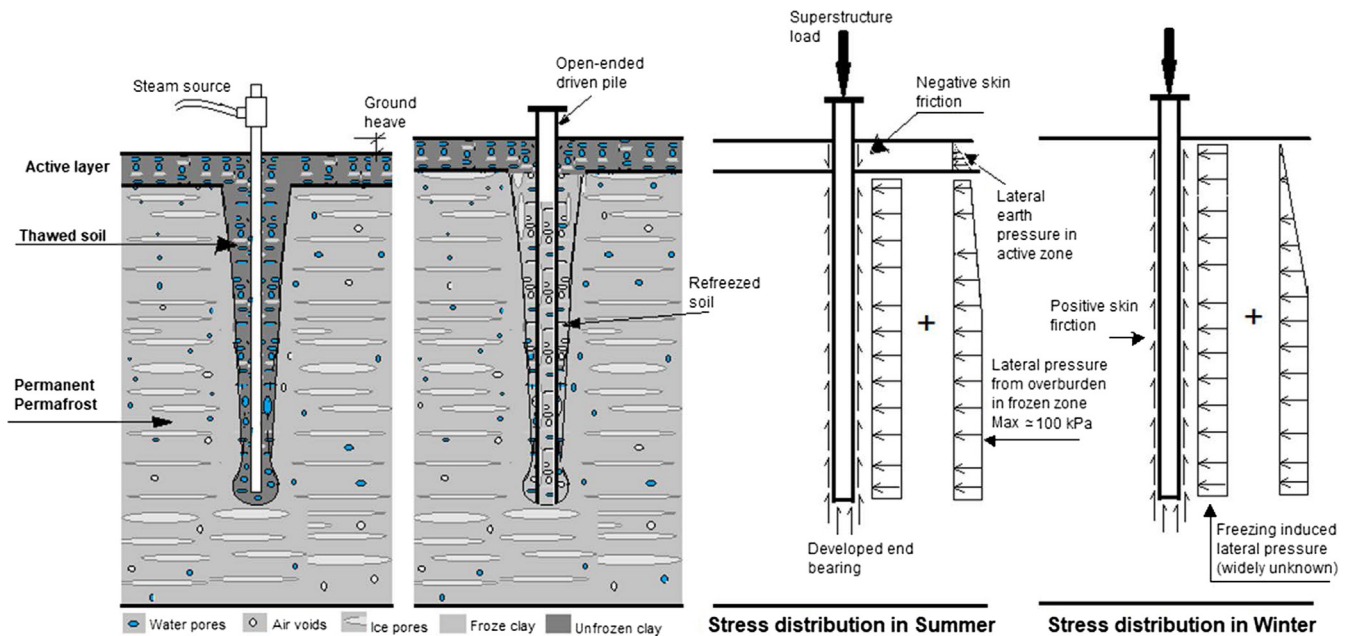
Fig. 8. Pile installation in pre-thawed soil and normal stress distribution from overburden and freeze-back pressure.
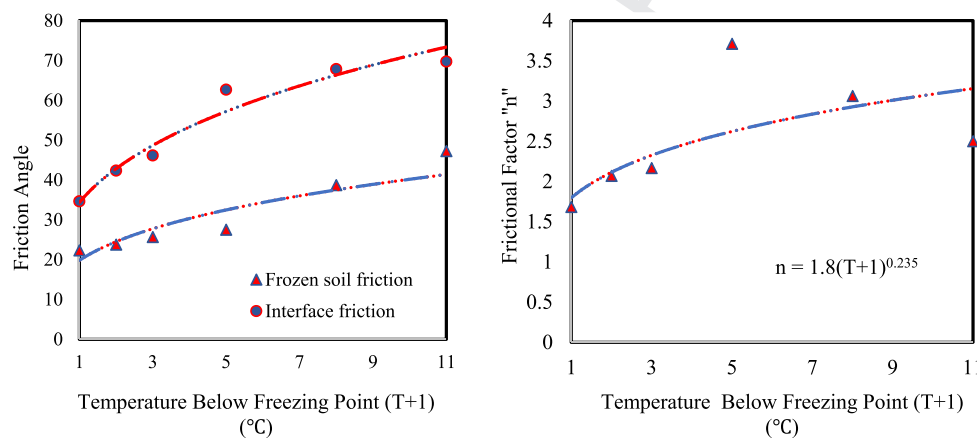

Fig. 9. (a) Variations in soil friction angle and pile-soil friction angle with temperature and (b) surficial frictional factor at different temperatures.

increasing normal stress. Moreover, fractured ice crystals contribute to the overall frictional resistance. At lower temperatures, therefore, higher friction angles were recorded due to higher ice contents. At temperatures lower than $-1°C$, the increasing normal stress was reported to slightly increase the unfrozen water content due to the pressure-melting effect (Jones 1982). The increase in the unfrozen water content would still be too small to reduce the adhesive and cohesive strengths as the temperature drops. However, the slight increase in the unfrozen water content was stated to bring the soil particles closer, resulting in higher frictional resistance. Due to the one-way drainage path system for the pile set-up, a higher amount of unfrozen water could accumulate at the predefined shear plane after soil refreezing around the piles compared to the two-way drainage path that formed in the frozen soils. Thus, higher frictional resistance and lower adhesive strength were recorded at the pile-soil interface compared to the friction angles and

the cohesive strength in frozen soils at any given temperature. The results obtained from the current experiment comply with the above-mentioned philosophy which was first proposed by Williams and Smith (1991). This has also been experimentally demonstrated in the present study.

The results generated from this study also support another statement made by Ladanyi and Theriault (1990) which suggests that the ultimate shaft capacity of piles may not only result from the adhesive strength, but also from the interface frictional resistance. Therefore, the contribution of frictional resistance should be implemented into the general equation used to estimate the shaft resistance of steel piles in frozen clay. In addition, since the normal stress resulted in larger interface friction, compared to the friction angles of frozen soils, a frictional factor "n" similar to the roughness factor "m" can be introduced to express the ratio $(\tan \delta)$ to $(\tan \varnothing)$ with respect to temperature. The frictional factor "n" versus temperature is pre-

sented in Fig. 9b. Although the data shows a scattered pattern, an exponential correlation could be proposed to express the variation in frictional factor "n" with positive values for the freezing temperatures plus unity (T + 1), as follows:

$$n = 1.80(T + 1)^{0.235} \qquad (8)$$

If the friction angle of frozen soil ($\varnothing$) is determined at any ground temperature (T) in the range of 0 °C to −10 °C, the frictional resistance of the steel piles installed in this frozen soil can then be expressed as

$$\tan(\delta) = 1.80(T + 1)^{0.235} \tan(\varnothing) \qquad (9)$$

Based on Eq. (9), the normal stress acting on steel piles in frozen clay could exert a frictional resistance that is at least 1.8 times greater than the frictional resistance exerted by frozen clay. This finding supports the hypothesis proposed by Ladanyi and Theriault (1990) which states that the horizontal stresses in frozen soils become greater than the initial state following the pile installation. This mobilized stress happens due to the frost heave associated with slurry refreezing or the soil freeze-back around the pile. However, the magnitude of the freezing-induced normal stress and the time required for the normal stress relaxation are still widely unknown and need more investigation preferably using a field set-up.

8.3. Theoretical estimation of ultimate shaft capacity of steel piles in frozen clay

The results from the current study confirm that using a constant roughness factor for predicting the adfreeze strength of steel piles in frozen ice-rich soils, as was adopted in previous design methods, could be very conservative, especially if the ground temperature is colder than −2°C. In practice, the load-carrying capacity of pile foundations depends on the shear strength parameters of the soil as well as the ground temperature and the loading rate. In this study, the shear strength parameters of the clay, the roughness factor, and the frictional factors were used to develop an empirical equation for predicting the ultimate shaft capacity of steel piles in frozen clay. The solution correlated the shear strength of frozen clay to the interface shear strength of steel piles through the modified roughness factor "m" and the introduced frictional factor "n". The ultimate shaft capacity was predicted based on the combination of the pile-soil adhesive strength and the interface frictional resistance both as a function of the freezing temperature and the strength parameters of the frozen clay, as follows:

$$\tau_a = 0.54(T + 1)^{0.215} C + 1.80(T + 1)^{0.235} \sigma_n \tan(\varnothing) \qquad (10)$$

where τ_a is the adfreeze strength of the steel piles in frozen clay at temperature T, σ_n is the total normal stress (kPa), C and $\varnothing$ are the cohesive strength (kPa) and the internal friction angle of the frozen clay at temperature T, respectively,

and T is the ground temperature as a positive degree Celsius value. For low permeable frozen clay, the total normal stress is a result of the overburden pressure and the refreezing-induced normal stress. Therefore, Eq. (11) can be written as follows:

$$\tau_a = 0.54(T+1)^{0.215} \ C + 1.80(T+1)^{0.235}(\sigma_{n_{overburden}} + \Delta\sigma_n)\tan(\varnothing) \qquad (11)$$

where $\sigma_{n_{overburden}}$ and $\Delta\sigma_n$ are the overburden pressure and the refreezing-induced normal stress, respectively.

9. Conclusion

A comprehensive experimental program has been carried out to investigate the performance of steel piles in ice-rich clay soils. The following conclusions can be drawn:

1- The ultimate shaft capacity of steel piles can be correlated to the shear strength of frozen clay using two surficial factors, namely, roughness factor "m" and frictional factor "n".
2- Roughness factor "m" is found to vary not only with the pile materials (e.g., steel, concrete, and timber), but also with the ground temperature and the stress conditions. This was attributed to the higher unfrozen water content accumulated in the vicinity of the pile-soil interface compared to regions far from the interface and might be linked to the different thermodynamic aspects between steel piles and clay soils.
3- Frictional factor "n", representing the ratio between the pile-soil interface frictional resistance and the frictional resistance of the frozen clay, was introduced in this study. The frictional factor decreases with an increasing freezing temperature, but it is always greater than unity and indicates a higher steel-soil frictional resistance at any given temperature or normal stress compared to the frictional resistance of frozen clay.
4- An empirical equation was provided for predicting the shaft resistance of steel piles in frozen clay soils. This equation would be more comprehensive upon obtaining information on the refreezing-induced normal stress and the normal stress from the overburden pressure in frozen ice-rich clay soils.

Uncited references

ASTM D5856–95 (2007), ASTM D698 (2012), Giraldo and Rayhani (2013), Ladanyi (1972).

Acknowledgements

References

Aldaeef, A.A., Rayhani, M.T., 2019a. Load transfer of pile foundations in frozen and unfrozen soft clay. Int. J. Geotech. Eng., 1–12

Aldaeef, A.A., Rayhani, M.T., 2019b. Load transfer and creep behavior of open-ended pipe piles in frozen and unfrozen ground. Innov. Infrastruct. Solut. https://doi.org/10.1007/s41062-019-0248-6.

Aldaeef, A.A., and Rayhani, M. T. (2017). Adfreeze strength and creep behavior of pile foundations in warming permafrost. Int. Cong. and Exh. "Sust. Civil Infra.: Innov. Infra. Geotechnology." Springer, Cham, 254-264.

ASTM D 4318. 2010. Standard Test Methods for Liquid Limit, Plastic Limit, and Plasticity Index of Soils. ASTM Int., West Conshohocken, PA, USA.

ASTM D3080/D3080M-11. (2012). Standard Test Method for Direct Shear Test of Soils Under 494 Consolidated Drained Conditions, Annual Book of ASTM Standards, ASTM Int., 495 West Conshohocken, PA. ASTM D422-63. (2007).

ASTM D422-63: Standard Test Method for Particle-Size Analysis of Soils, Annual Book of 484 ASTM Standards, ASTM Int., West Conshohocken, PA, 2007.

ASTM D5321-12. (2014). Standard test method for determining the shear strength of soil-geosynthetic and geosynthetic-geosynthetic interfaces by direct shear, ASTM Int., West Conshohocken, PA.

ASTM D5856-95, 2007. Standard Test Methods for Measurement of Hydraulic Conductivity of Porous Materials using a Rigid-Wall Compaction-Mold Permeameter. West Conshohocken, PA: ASTM International, https://doi.org/10.1520/D5856-95R07.

ASTM D698. (2012). Standard Test Methods for Laboratory Compaction Characteristics of Soil Using Standard Effort (12 400 ft-lbf/ft3 (600 kN-m/m3), West Conshohocken, PA: ASTM Int., DOI:10.1520/D0698-12.

Biggar, K.W., Sego, D.C., 1993. Field pile load tests in saline permafrost. I. Test procedures and results. Can. Geotech. J. 30 (1), 34–45.

Crory, F. E. (1963). Pile foundations in permafrost. Proc., 1st Permafrost Int. Conf., Lafayette, Indiana, NAS-NRC Publ. No. 1287, 467-472.

Crory, F.E., Reed, R.E., 1965. Measurement of Frost Heaving Forces on Piles. Cold Reg. Res. Eng. Lab. Technical Report, p. 145.

Dalmatov, B.I., Karlov, V.D., Turenko, I.I., Ulitskiy, V.M., and Kharlab, V.D. (1973). Interaction of freezing heaving with foundations. Proc. 2nd Int. Conf. on Permafrost, Yakutsk, USSR Contribution, National Academy Press, Washington, DC, 572-576.

Giraldo, J., Rayhani, M.T., 2013. Influence of fiber-reinforced polymers on pile–soil interface strength in clays. Adv. Civil Eng. Mater. 2 (1), 1–17. https://doi.org/10.1520/ACEM20120043, ISSN 2165-3984.

Johnson, J.B., & Buska, J.S. (1988). Measurement of frost heave forces on H-piles and pipe piles (No. CRREL-88-21). Cold Reg. Res. Eng. Lab, Hanover, NH.

Johnston, G.H., Ladanyi, B., 1972. Field tests of grouted rod anchors in permafrost. Can. Geotech. J. 9 (2), 176–194.

Jones, S.J., 1982. The confined compressive strength of polycrystalline ice. J. Glaciol. 28 (98), 171–177.

Kitze, F.F. (1957). Installation of piles in permafrost. Cold Reg. Res. Eng. Lab, Arctic construction and frost effects laboratory, Corps of Engineers, U.S. Army.

Ladanyi, B., 1972. An engineering theory of creep in frozen soils. Can. Geotech. J. 9 (1), 63–80.

Ladanyi, B., Theriault, A., 1990. A study of some factors affecting the adfreeze bond of piles in permafrost. Int. Proc. Geotech. Eng. Cong. GSP 27, 213–224.

Ladanyi, B., 1988. Short- and long-term behavior of axially loaded bored piles in permafrost. In: Proc. of Int Symp. Deep Found. on Bored and Auger Piles. Ghent. Belgium, pp. 121–131.

McQueen, W., Miller, B., Mayne, P. W., & Agaiby, S. (2015). Piezocone dissipation tests at the Canadian test site No. 1, Gloucester, Ontario. Can. Geotech. J. 53(5), 884–888.

Morgenstern, N.R., Roggensack, W.D., Weaver, J.S., 1980. The behavior of friction piles in ice and ice-rich soils. Can. Geotech. J. 17 (3), 405–415.

Nixon, J.F., 1978. Foundation design approaches in permafrost areas. Can. Geotech. J. 15 (1), 96–112.

Nixon, J.F., 1988. Pile load tests in saline permafrost at Clyde river, northwest territories. Can. Geotech. J. 25 (1), 24–32.

Nixon, J.F., McRoberts, E.C., 1976. A design approach for pile foundations in permafrost. Can. Geotech. J. 13 (1), 40–57.

Parameswaran, V.R., 1978. Adfreeze strength of frozen sand to model piles. Can. Geotech. J. 15 (4), 494–500.

Parameswaran, V.R., 1979. Creep of model piles in frozen soil. Can. Geotech. J. 16 (1), 69–77.

Parameswaran, V.R., 1981. Adfreeze strength of model piles in ice. Can. Geotech. J. 18 (1), 8–16.

Parameswaran, V.R., 1987. Adfreezing strength of ice to model piles. Can. Geotech. J. 24 (3), 446–452.

Penner, E., 1970. Frost heaving forces in Leda clay. Can. Geotech. J. 7 (1), 8–16.

Penner, E., 1974. Uplift forces on foundations in frost heaving soils. Can. Geotech. J. 11 (3), 323–338.

Penner, E., Gold, L.W., 1971. Transfer of heaving forces by adfreezing to columns and foundation walls in frost-susceptible soils. Can. Geotech. J. 8 (4), 514–526.

Penner, E., Irwin, W.W., 1969. Adfreezing of Leda clay to anchored footing columns. Can. Geotech. J. 6 (3), 327–337.

Sego, D.C., Smith, L.B., 1989. Effect of backfill properties and surface treatment on the capacity of adfreeze pipe piles. Can. Geotech. J. 26 (4), 718–725.

Ting, J.M., 1981. The creep of frozen sands: qualitative and 279 quantitative models – final report II. In: U.S. Army Res. Office, Res. Rep., N, pp. R81–R85.

U.S. Army/Air Force. (1967). "Arctic and subarctic construction: structure foundations." Tech. Manual TM5-852-4/ AFM 88-19, chap. 4.

Vialov, S.S. 1959. Rheological properties and bearing capacity of frozen soils. Transl. 74, US Army Cold Reg. Res. Eng. Lab, Hanover, N.H. 1965.

Viggiani, G., Ando', E., Takano, D., Santamarina, J., 2015. Laboratory X-ray tomography: a valuable experimental tool for revealing processes in soils. Geotech. Test. J. 38 (1), 61–71.

Voitkovskii, K.F. (1960). Mekjanicheskiye svoystva lda. Izvestiya Akademii Nauk, Moscow. [The mechanical properties of ice. U.S. Air Force Cambridge Res. Lab., Bedford, Mass., Translation No. AFCRL-62–838.].

Wang, J., Nishimura, S., Tokoro, T., 2017. Laboratory study and interpretation of mechanical behavior of frozen clay through state concept. Soils Found. 57 (2), 194–210.

Weaver, J.S., Morgenstern, N.R., 1981. Pile design in permafrost. Can. Geotech. J. 18 (3), 357–370.

Williams, P.J., Smith, M.W., 1991. The Frozen Earth: Fundamentals of Geocryology. Cambridge, U.K..